Reassembling Waste: Towards a Carbon Zero Built Environment

Luis Santos[1][0000-0002-2664-4301] and Inês Caetano[2][0000-0003-3178-7785]

[1] Department of Architecture, Design and Media Technology, Aalborg University, Aalborg, Denmark
[2] Department of Computer Science and Engineering, INESC-ID, Instituto Superior Técnico, University of Lisbon, Lisbon, Portugal
[1]lfds@create.aau.dk

Abstract. The building sector is a major contributor to greenhouse gas emissions. Therefore, reducing construction activities' global warming potential (GWP) is essential in mitigating the sector's environmental impact. This work presents a novel Performance Generative Design System (PGDS) to promote circular design processes towards low-carbon architecture. The PGDS supports architectural design workflows that aim the reuse of building materials in the creation of low-carbon structures. Using a co-simulation approach, the PGDS integrates validated Life Cycle Analysis (LCA) and Building Energy Simulation (BES) tools to evaluate environmental impacts, and includes a custom packing algorithm to optimize material reuse. The system's modular structure allows flexible application to various design scenarios, enhancing the potential for performance-based, low-GWP building designs. The authors tested the system in a hypothetical design of a 4-story office building located in Horsens, Denmark. The proposed PGDS generated designs that maximize building material waste usage and minimize building energy consumption and cradle-to-grave GWP, resulting in up to 18% savings of CO_2 equivalent emissions. Finally, the authors discuss the current limitations of the PGDS related to its packing and material distribution abilities and building performance criteria to suggest future improvements.

Keywords: Circular economy in design and construction, building waste reusage, life cycle assessment, algorithmic design, performance-based design.

1 Introduction

The building sector alone is responsible for 37% of global anthropogenic greenhouse gas emissions associated with climate change and global warming [1]. Reducing construction activities' global warming potential (GWP) is thus imperative, motivating architectural design practices to incorporate life cycle analysis (LCA) methods to guide low-carbon design.

LCA is a method that quantifies the environmental impact of a product, system, or service throughout its life cycle, examining inputs (e.g., materials, energy), processes (mechanical or chemical), and outputs (e.g., emissions, waste). It uses indicators covering environmental impact, resource use, waste and emissions, toxicity, and biodiversity. GWP is an environmental impact indicator typically expressed in kg CO_2-eq. In the building industry, LCA data for materials is available through Environmental Product Declarations (EPDs) or generic LCA databases for early design phases [2]. LCA encompasses four phases: production and construction (A), use, operation and maintenance (B), end-of-life (C), and reuse, recovery, or recycling (D).

Besides LCA, interest is growing in designing buildings for disassembly [3] and reusing building waste materials or components in new structures [4–6]. These strategies align with the broader framework of circular design, which reduces waste and maximizes resource efficiency by reusing and recycling materials [7]. Additionally, architects are also focusing on the carbon sink potential of bio-based materials for decarbonization [8,9] exploring their tectonic and architectural expression [10,11]. However, reuse of waste materials remains limited in practice, with exceptions including Villa Welpeloo by Superuse Studios, the Open-air Library Salbke by KARO architects, and Resource Rows housing complex by Lendager Group and Arkitektgruppen [3].

There are challenges in integrating LCA tools with current architectural design workflows, as they often lack compatibility with digital and computational design methods. Exceptions include Bombyx [13], One-click LCA, and Rhino Circular [14], which interface with standard Computer-aided Design (CAD) and Building Information Modeling (BIM) packages. Additionally, there is insufficient information on the availability, quality, and certification processes for reusing building products, leading to increased costs and complexity. Professional training in construction waste reuse needs improvement to address the prevailing lack of awareness and openness toward material reuse [12].

Furthermore, the LCA methodology still lacks clear approaches for the reuse/recycle phase (Phase D), often excluded from system boundaries. While standards like ISO 21930 [15], EN 15804 [16] and the European Commission guidance for Product Environmental Footprint Category Rules [17] address the net benefits and loads of reused materials in LCA's Phase D, they vary in depth and detail, leading to a lack of a unified framework, especially for calculating the GWP of reused materials in buildings.

Lastly, the architectural discipline still lacks a strong culture around the tectonic and aesthetic potential of waste reuse. Fortunately, projects like Resource Rows have increased interest in material circularity, motivating critical think-tanks like Circular[x]Change [18], representing the rise of a culture focused on material reuse in architecture.

2 Research goals

This work addresses some of the challenges discussed, particularly those related to circularity in the design process. The aim is to develop a framework that can leverage different computational design processes, cradle-to-grave LCA calculations, and Building Energy Simulation (BES) to enhance performance-based design processes that embrace material circularity in the creation of low-carbon buildings. The target outcome is a novel Performance-based Generative Design System (PGDS) that facilitates the reuse of building demolition waste in new structures. By empowering architects to design low-carbon structures, such PGDS aims to promote awareness and support the development of a tectonic discourse fully embracing the concept of waste.

3 Methodology

The investigation followed a methodology composed of four stages. The first stage, summarized in Section 1, involved an analysis of the state-of-the-art on circular building design and material reuse in architecture to identify current challenges and needs.

The second stage focused on defining the framework structure, supported strategies, and design workflows, along with designing the PGDS architecture.

The third stage entailed implementing the PGDS using Khepri [19], an algorithmic design tool based on the Julia programming language and portable across different CAD/BIM tools, and Grasshopper, Rhino3D's visual programming language, and its front-ends to the BES tool EnergyPlus [20].

The last stage evaluated the PGDS in different design experiments.

3.1 Performance-based generative design system

The PGDS integrates validated LCA and BES tools along with a custom packing algorithm for design workflows that aims to efficiently and innovatively reuse building materials/components from material banks or atlas. Fig. 1 presents its structure and data flows.

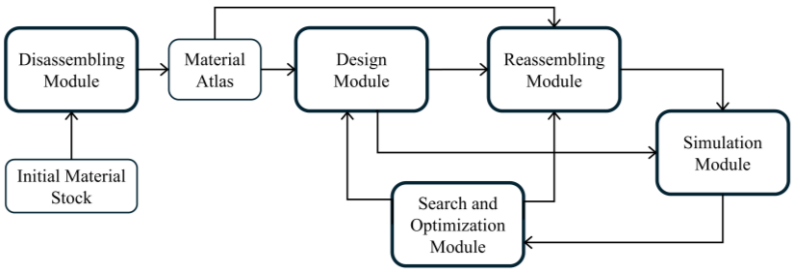

Fig. 1. The PGDS modules and potential interactions and data flowchart.

By evaluating environmental impacts across different materials, building forms, envelope designs, and operational performance, the PGDS enhances performance-based design workflows for low-carbon buildings. The leverage of algorithmic strategies, LCA, and BES makes it a robust and versatile tool for designing low-GWP buildings, supporting the green transition of the built environment and enhancing resource efficiency. Additionally, it allows architects to explore the tectonic potential of reusing building material waste more easily and efficiently.

The PGDS modular structure ensures a flexible application to different design tasks and scenarios. For example, if a material atlas is already available, there is no need to use the disassembling module. Also, if architects want to explore one-at-a-time design solutions, there is no need to use the search and optimization module. Alternatively, if they wish to find better-performing solutions, they should use the design module to create the parametric description of the design for the search and optimization module.

The following sections describe each module and related approaches in detail.

Disassembling module. This module divides a building or its components into smaller, reusable elements using a simple disassembly logic based on pre-labeled component descriptions that provide essential semantics (type of element) and geometric information. Fig. 2 illustrates the disassembly process for an existing wall with two fenestrations.

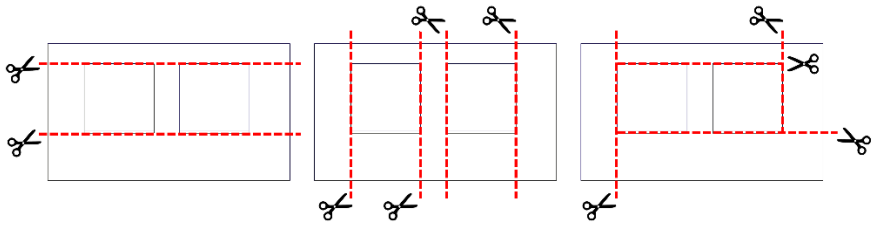

Fig. 2. Conceptual representation of the disassembling module logic in a façade with two fenestrations.

In this module, the user specifies whether the building component will be cut vertically, horizontally, or in both directions. Additionally, the user can constrain the length-to-width ratio of the final pieces to avoid overly slender material fragments. The disassembly module then cuts the component based on the fenestration sides accordingly while grouping and labeling the resulting fragments by ID and material type into a material atlas.

Design module. The design module supports the parametric description of building surfaces or parts that integrate reused/reclaimed building materials or elements. Users define the building surface and specific sub-areas for placing certain elements—e.g., windows—or no element—e.g., stair cores in slabs, façade or roof

openings, or existing elements that cannot overlap. Additionally, users can constrain recycled element placement to achieve goals like a target glazing area or window-to-wall ratio (WWR) for a façade.

Based on the WWR, the design module generates multiple window sets using a custom algorithm that considers surface area, the window atlas, and the target WWR. It returns a list of windows with the achieved glazing area and WWR, enabling users to verify metrics and update the material atlas. This functionality supports an efficient exploration of window combinations aligned with different design concepts, spatial functions, structural grids, or cladding panel sizes.

After selecting the window set, users can linearly distribute the windows along the defined area(s) using another algorithm (Fig. 3A). The algorithm receives the list of windows to distribute, the placement area(s), and an increment value for adjusting the windows' y-axis positions. It then distributes the windows along the area(s)' length, applying equal or random spacings and vertical shifts in increments of the specified value. If the increment is zero, the window height remains constant. Alternatively, the windows can be packed within user-defined areas (Fig. 3B) using the custom packing algorithm explained in the next section.

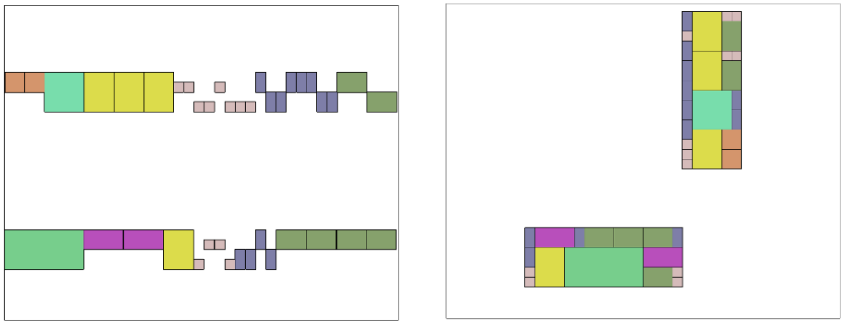

Fig. 3. The same window set distributed linearly with vertical shifts randomly varying between two positions (A) or packed within user-defined areas (B). Each window type (ID) is color-coded.

Reassembling module. This module facilitates the packing of building elements based on user-defined constraints, such as allocation area(s), material atlases, and target metrics, including overall WWR for façades or varying WWRs for specific areas. Allowing users to control building element placement by selecting elements, defining material allocation areas, and determining targets for WWR supports designers in meeting architectural requirements related to privacy, thermal performance, and lighting. Using such information, the reassembling module explores various material allocation configurations.

At its core, the reassembling module uses a custom packing algorithm, which takes the list of elements to be packed and the area to cover. Additionally, it can receive a list of sub-areas to avoid and a Boolean value indicating whether elements

can rotate during packing. Based on this information, the algorithm arranges the elements within the allowed area(s), reducing gaps between them. The result is a list of placed elements with details about each element's typology (ID), dimensions, and placement locations.

This information facilitates material coverage calculations and the extraction of construction data. Additionally, it enables visualization of packing results in a modeling tool, where each element type (ID) is assigned to different layers, colors, or materialities. To support these capabilities, the reassembling module includes additional custom algorithms for analyzing, storing, and manipulating packing data.

Fig. 4 illustrates two functionalities: on the left, a visualization of the packing result that shows the resulting pattern while clearly distinguishing different element typologies; on the right, a spreadsheet presents numerical packing data, associating element IDs with their dimensions and placement locations for easy reference and analysis.

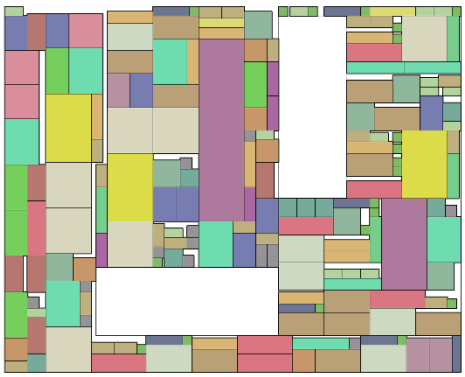

Typology (ID)	Length cm	Width cm	X	Y
B15	50	25	0	20
B18	40	40	350	250
BR1	120	40	750	700
BR3	60	60	750	550
C15	100	50	600	100
BR2	100	60	600	200
B15	50	25	750	775
C17	100	25	750	500
C15	100	50	750	450
BR7	40	20	625	800
C18	75	100	425	250
BR4	80	20	600	150
BR1	120	40	750	400
C14	100	100	225	250
C20	50	75	500	250
B18	40	40	50	20
C14	100	100	870	700
C23	125	25	750	675
C15	100	50	810	550
C15	100	50	750	610
B13	50	50	0	45
BR9	25	25	575	250
C15	100	50	700	100
C15	100	50	700	150
C23	125	25	700	200
BR2	100	60	600	260
C16	100	200	425	350

Typology	Amount
BR5	4
C20	8
BR3	7
B15	19
B14	3
BR8	20
C16	3
C23	4
C13	3
B17	6
C19	3
C22	4
C15	12
BR1	8
BR2	6
BR7	15
C18	6
C17	11
BR9	15
B18	8
BR4	7
B16	5
C14	7
B13	6
BR6	2

Fig. 4. Left: Packing results visualized in a modeling tool, with each color representing an element type (ID). Right: Packing results are presented numerically, with each data element organized by row.

The reassembling module includes an optimization algorithm based on a Monte Carlo-based search strategy [21] to balance area coverage maximization with existing design requirements. This algorithm searches for the packing configuration that minimizes unfilled spaces within the defined constraints. Suppose the available material atlas is insufficient to cover the designated area. In that case, the user can either stop the packing process when no more elements are available or continue by incorporating new elements. The user can directly provide these new elements via a new material atlas, or the algorithm can automatically generate them using the original atlas as a reference. In the latter case, the algorithm assigns a unique ID to each element, prefixed with "new" (e.g., new_Br01), to distinguish it from existing elements.

Fig. 5 presents three packing configurations for a rectangular façade produced by the reassembling module with different material atlas and material allocation areas.

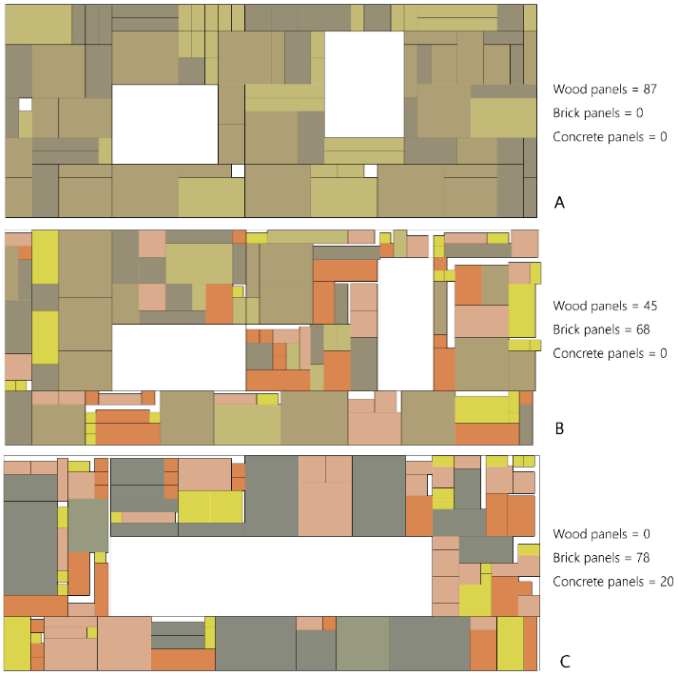

Fig. 5. Three packing configurations for the same façade using different panel sets and designated areas without panels: A. only wood panels; B. wood and brick panels; C. brick and concrete panels.

Simulation module. This module integrates two building simulation methods: dynamic BES via EnergyPlus' frontend ClimateStudio [22] and cradle-to-grave LCA analysis via Bombyx, a Grasshopper plugin for early-stage LCA.

The first method, BES, allows the optimization of other module inputs (e.g., WWR to minimize energy consumption) and the calculation of the operational energy of any design solution. To estimate building energy related carbon emissions, the tool supports the conversion of energy (kWh) into GWP emissions (kg CO2-eq) using energy emission factors, which can be either provided by the user or automatically estimated based on the building's location and the source energy type for different end-uses (e.g., heating, cooling, lighting, etc.). Such converted values are critical for LCA Phase B6 (Operational Energy) GWP estimations.

The second method supports LCA calculations across the following phases:

- Phase A – Production: A1 (raw material extraction), A2 (transport), A3 (manufacturing)

- Phase B – Use, maintenance, and operation: B4 (replacement), B6 (operational energy use, from BES)
- Phase C – End of life: C3 (waste processing), C4 (disposal)

Phase D (post-end-of-life) is indirectly considered through material reuse from the building's material atlas, with GWP calculations for reused materials excluding Phases A1-A3. The module assumes a worst-case end-of-life scenario for reused materials, treating them as waste. The building's LCA life period is 50 years, and the module estimates circularity potential by estimating CO_2-eq savings from reused materials compared to new ones.

To perform the simulations, users must specify key inputs.

For the first method (BES), the required inputs include: (1) the site's typical meteorological year (TMY) in an EnergyPlus weather file (**.epw*); (2) information on internal loads, heating, ventilation, and air-conditioning (HVAC) systems, and deployed passive design strategies (e.g., natural ventilation and dynamic shading); and (3) lighting, occupancy, and equipment profiles. Thermal and optical material properties (e.g., U-value, VLT, and SHGC) are typically sourced from the material atlas. Users only need to provide these values if the material is missing from the ClimateStudio and Bombyx databases.

For the second method (LCA), users must provide material quantities and building element types. Bombyx's LCA databases provide GWP values based on the specified materials. Nevertheless, it is also possible to outsource data related to cradle-to-grave GWP of different materials and building products from an environmental product declaration (EPD).

Search and optimization module. Since the PGDS implementation is in Julia and Grasshopper, it can leverage optimization packages available in both programming languages, such as Julia's *metaheuristic.jl* [23] and Grasshoppers' native optimizers (i.e., simulated annealing and standard genetic algorithm). These tools enable the PGDS to automatically search for solutions that optimize a user-defined objective function along with equality and/or inequality constraints.

Typically, optimization focuses on minimizing building energy consumption, cradle-to-grave GWP, or both. However, additional environmental key performance indicators, such as daylight-related metrics, might also be included.

3.2 Design of Experiments

We tested the PGDS in two experiments based on a real-world case: the planned urban transformation in Horsens, Denmark, which involves the demolition of some residential buildings in the Sundparken social housing complex (Fig. 6 [24]). These experiments are face validity tests [25], assessing whether the proposed PGDS relies on plausible assumptions and produces explainable, meaningful, and architecturally relevant outcomes.

Both experiments consider the site's climate and use the material atlas resulting from the planned Sundparken demolitions to design a medium-sized, four-story

office building within the broader urban proposal proposed in [24]. The box-shaped building has a north-south orientation, glazed façade areas on the north and south, and solid gable walls on the east and west.

Experiment 1 investigates two WWR alternatives for the south and north façades, iteratively testing various insulation materials to meet a target U-value while assessing their impact on overall GWP. The aim is to evaluate the PGDS's ability to support performance-based, iterative design explorations where architects compare design solutions regarding material allocation, energy performance, cradle-to-grave GWP, and construction circularity potential.

Experiment 2 begins by pre-optimizing the building's shape, WWR for south and north façades, and the U-values of different building envelope surfaces to reduce operational energy consumption. The pre-optimized shape and WWR then inform the reassembly process, while the pre-optimized U-values guide a second optimization step to select an envelope material assemblage that further minimizes GWP. The aim is to assess the PGDS's ability to support goal-oriented design processes, assisting designers in efficiently exploring the design space and achieving high-performing solutions.

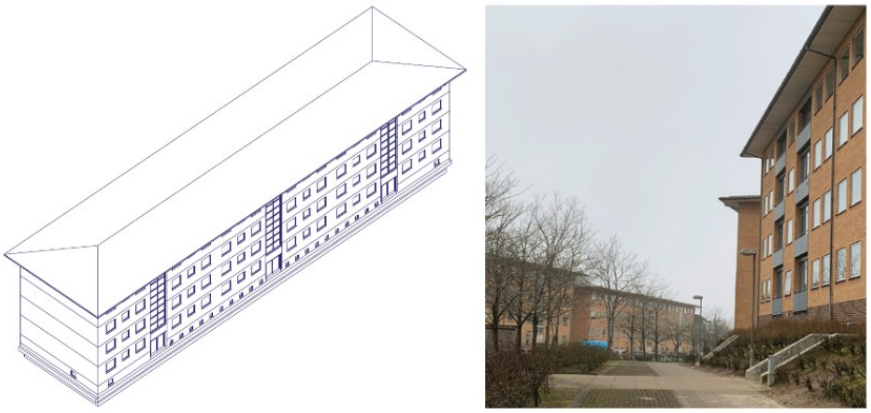

Fig. 6. A building block typology to be demolished in Sundparken, Horsens, Denmark. Left: axonometric. Right: street view (Source: [24]).

Both experiments use only 33% of the material atlas, based on the assumption that its content is evenly distributed across all new buildings of the urban development proposed in [24]. Table 1 shows the material atlas used in the experiments, and Fig. 7 illustrates its structure.

Table 1. Material atlas used in the two experiments.

Building component	Typologies	Quantity
Double-glazed insulated windows	9	52
Concrete panels (heavy sandwich, single lightweight, and hollow panels)	31	399
Composite panels (heavy sandwich concrete + brick veneer panels)	2	96
Brick panels	14	153

	A	B	C	D	E	F	G	H	I
1	ID	Material	Type	Width (m)	Height (m)	Thickness	Quantity	Extra info	
2	W1	Glazing	Window	2.25	1.9	0.06	4.00	Fixed	
3	W2	Glazing	Window	2.25	0.55	0.06	1.00	Fixed	
4	W3	Glazing	Window	2.1	1.35	0.05	8.00	Tilt and Turn	
5	W4	Glazing	Window	2.95	2.25	0.12	8.00	Sliding	
6	W5	Glazing	Window	2.7	1.3	0.06	18.00	Tilt and Turn	
7	W6	Glazing	Window	2.00	1.00	0.06	4.00	Tilt and Turn	
8	W7	Glazing	Window	2.15	1.2	0.06	1.00	Top Hung	
9	W8	Glazing	Window	0.75	1.3	0.06	4.00	Top Hung	
10	W9	Glazing	Window	0.9	0.45	0.06	4.00	Fixed	
11	C1	Concrete	Sandwich	1.2	2.8	0.25	48.00	Gable element	
12	C2	Concrete	Sandwich	1.2	0.3	0.25	48.00	Gable element	
13	C3	Concrete	Sandwich	2.4	1.35	0.25	5.00	Heavy concrete element	

Fig. 7. Part of the material atlas used in both experiments organized in a spreadsheet.

Besides the material atlas, the experiments follow the same construction scheme for exterior walls, ground, floors, and roof, as presented in Table 2. They also share key BES parameters, namely:

- Site's TMY data (Horsens, Denmark).
- Double-glazed window properties: U-value of 1.60 W/m^2.K, a SHGC of 0.75, and VLT of 0.65.
- An Ideal Load Air System (ILAS)[1] HVAC system with heating and cooling setpoints set as 20°C and 26°C, respectively.

Table 2. Construction scheme for different building surfaces.

Layers #	Exterior walls	Ground floor	Intermediate floors	Roof
1 (outermost)	Reused brick or concrete or oak wood for new cladding	Polymer bitumen membrane water barrier	Reused or new wood parquet	Recycled concrete ballast (sourced on site)

[1] ILAS is an ideal variable air volume (VAV) terminal system that supplies heating and cooling air to meet the heating or cooling loads of different thermal zones.

2	Ventilated air gap	Insulation to-be-determined (TBD)	Cross-laminated Timber (CLT) 220 mm	Polymer bitumen membrane water barrier
3	Air barrier in Oriented Strand Board (OSB)	Polythene vapor barrier	-	Insulation TBD
4	Insulation TBD	Exposed concrete slab	-	Polythene air/vapor barrier
5	Polythene water/vapor barrier	-	-	CLT 220 mm
6	CLT 220 mm	-	-	-
7 (innermost)	Gypsum board	-	-	-

Danish regulations mandate minimal use of active cooling during the summer to promote energy conservation. The simulations employ dynamic shading, deploying exterior Venetian blinds when the incident radiation on windows exceeds 200 W/m2 to comply with such regulations. Additionally, the simulation process enables cross-natural ventilation when the indoor operative temperature exceeds 22°C, the outdoor temperature is between 15°C and 30°C, and the relative humidity is below 90%. Table 3 describes the internal energy loads considered in both experiments.

Table 3. Assumptions for internal loads used in building energy simulations.

People (ppl)	Equipment	Lights
0.2 ppl/m^2 with a typical office occupancy schedule	9.4 W/m^2 with a typical office schedule	6.6 W/m^2 - dimmable LED system with illuminance target set to 300 lux

The experiments account for Horsens' heating supply, based on an efficient central district system that reuses heat from industrial processes, to calculate the building's operational energy GWP. Thus, we used a carbon emission factor of 0.05 $kgCO_2$-eq./kWh [26]. For all other building energy end-uses that rely on electricity, we assumed a carbon emission factor of 0.138 kgCO2-eq./kWh [26].

4 Results

This section describes the two experiments conducted using the PGDS.

4.1 Experiment 1

This experiment tested the PGDS's ability to support performance-based, iterative design processes, facilitating the exploration of material and assembly combinations while ensuring specific envelope properties like WWR and U-value. The design workflow started with users specifying the building part(s) to modify and the material atlas to apply. Users then applied a standard and alternative WWR to the defined building part(s) for comparison. Specifically, the experiment used the office building's south and north façades (22.8x13.2 m), the Table 1 material atlas, a U-value of 0.15 W/m^2.K for the opaque envelope portion, and a WWR of 40% [27,28] in both façades (standard scenario) or 50% and 30% in the south and north façades, respectively (alternative scenario).

The design workflow continued with users applying the PGDS to generate different solutions for each scenario. Using the design module, users parametrically defined the envelope surfaces for allocating reused windows and calculating one or more window sets that meet the established WWR values. Additionally, users specified areas for placing these window sets. In the standard scenario, specific regions contain windows on both façades. In the alternative scenario, specific areas on the south façade contain the windows, while the arrangement of windows in the North façade is linear, i.e., side by side.

The next step used the PGDS to maximize material reuse. Using the reassembling module's optimization and packing algorithms, users automated the search for the design configuration that maximizes façade coverage with reused elements. To that end, the system produced and examined 1500 iterations. The reassembly module also provides detailed information on the quantities of different reused material types, which is crucial for LCA calculations. Fig. 8 shows the best packing configuration for each scenario, and Table 4 presents the corresponding results.

Fig. 8. Best packing configurations achieved in experiment 1 for scenarios 1 (40-40 WWR) and 2 (50-30 WWR): light blue represents the reused windows, textured grey represents concrete panels, the brick texture illustrates the brick panels, and the wood texture indicates the use of new wood cladding.

Table 4. Material distribution for both design scenarios of experiment 1.

	Standard scenario (40-40% WWR)			Alternative scenario (50-30% WWR)		
	South	North	Total	South	North	Total
Reused windows	39	9	66%	43	8	64%
New windows	0	25	34%	0	29	36%
Reused Panels	164	65	86.5%	128	88	87%
Void Area	27 m^2	54 m^2	13.5%	24.4 m^2	54 m^2	13%

Then, users explored different insulation materials and thicknesses to achieve the U-value of 0.15 $W/m^2.K$ for the various envelope surfaces. Table 5 presents the results for three insulation materials: (i) woodfiber, (ii) cellulose, and (iii) expanded polystyrene (EPS). The ground slab and roof could not use cellulose insulation batt due to its weight and poor moisture performance on horizontal surfaces.

Table 5. Different types of insulation materials and correspondent thicknesses for different building surfaces.

Insulation material	Conductivity λ (W/m.k)	Thickness for Ground (mm)	Thickness for Walls (mm)	Thickness for Roof (mm)
Wood fiber	0.042	260	200	200
Cellulose	0.042	N.A.	200	N.A.
EPS	0.035	220	180	180

Lastly, using the information on insulation materials and the quantities of reused materials, users calculated the operational energy use intensity (EUI – kWh/m^2) and cradle-to-grave GWP (kg CO_2/m^2 year) for each insulation material variation in each design scenario using the simulation module. Table 6 presents the results.

Table 6. Experiment 1 final EUI and GWP results.

	Standard scenario: 40-40% WWR			Alternative scenario: 50-30% WWR		
Insulation type	Wood Fiber	Cellulose	XPS	Wood Fiber	Cellulose	XPS
GWP (reusing materials) (kg CO_2/m^2year)	11.8	11.7	12.8	11.6	11.5	12.5
GWP (new materials) (kg CO_2/m^2year)	12.9	12.7	14.3	12.6	12.5	14
EUI (kWh/m^2year)	118			115		

4.2 Experiment 2

To minimize operational energy consumption, users used a standard genetic algorithm, which ran for 100 generations, each with a population of 100 design variations, to pre-optimize the building shape, WWR of the north and south façades, and the U-values for various envelope surfaces (ground, exterior walls, and roof). Table 7 describes the decision variables, while Table 8 presents their pre-optimized values.

Table 7. Decision variables of the pre-optimization process conducted in experiment 2.

Variable	Domain	Type	Comments
Length (m)	[11.4, 34.2]	Discrete	Steps of 5.7 m*
Width (m)	[10.8, 18]	Discrete	Steps of 1.2 m*
WWR south (%)	[0.1, 0.95]	Discrete	Steps of 5%
WWR north (%)	[0.1, 0.95]	Discrete	Steps of 5%
U-value ($W/m^2.K$)			
Exterior walls	[0.07, 0.25]	Continuous	-
Roof	[0.07, 0.25]	Continuous	-
Ground floor	[0.1, 0.3]	Continuous	-
* due to potential reuse of existing elements			

Table 8. Pre-optimized values in experiment 2.

Design Variable	**Pre-optimized Value**
Building Shape	
South & North Façades	34.2 x 13.2 m
East & West Gables	14.4 x 13.2 m
WWR	
South Façade	60%
North Façade	10%
U-Value	
Exterior Walls & Roof	0.07 $W/m^2 \cdot K$
Ground Floor	0.1 $W/m^2 \cdot K$

The design workflow continued as described in section 3.1, now using the pre-optimized results. Due to the need to achieve a higher WWR on the south façade, the area defined for window allocation was increased by 2 meters in length. Fig. 9 shows the best panel packing for two alternative window configurations for both

façades, while Fig. 10 presents rendered southeast and northwest perspectives, and Table 9 reports the corresponding results.

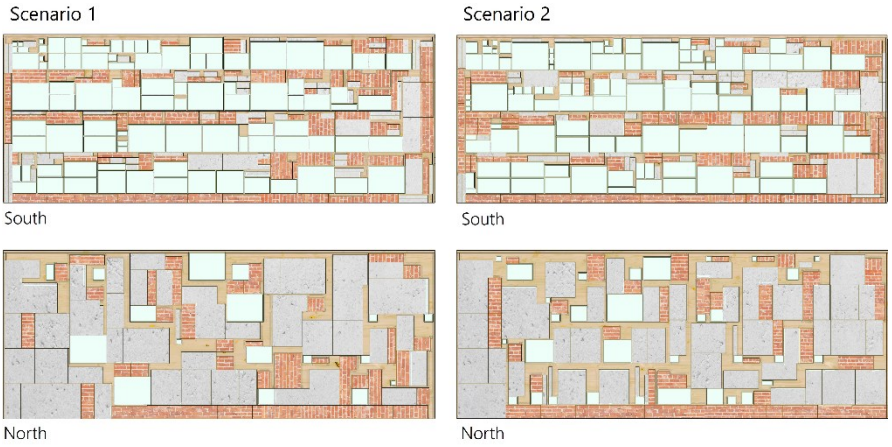

Fig. 9. The best panel packing after 1500 iterations for two window sets in both south and north façades: light blue represents the reused windows, and the textured grey and orange elements represent the reused concrete and brick panels, respectively, and the wood texture indicates the use of new wood cladding.

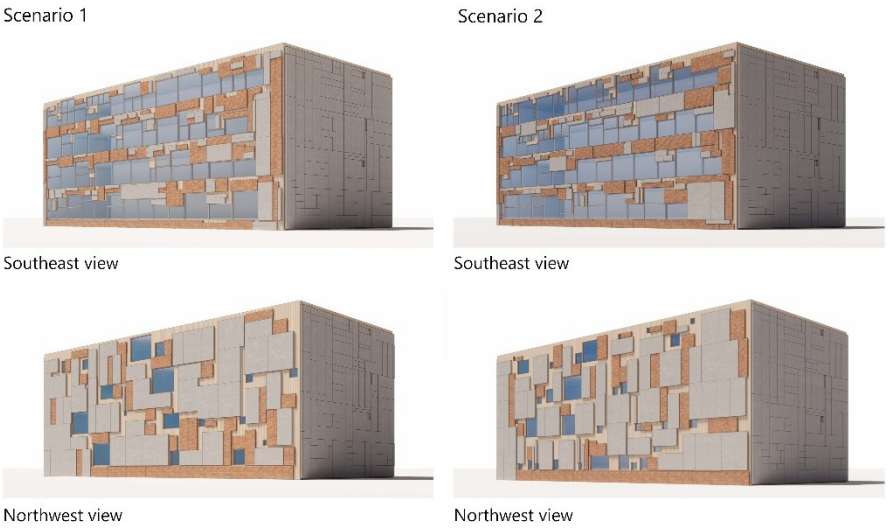

Fig. 10. Perspective views of the best design solutions found in experiment 2.

Table 9. Material distribution for both design scenarios of experiment 2.

	Scenario 1 (60-10% WWR)			Scenario 2 (60-10% WWR)		
	South	North	Total	South	North	Total
Reused windows	51	1	66%	52	0	64%
New windows	41	16	34%	50	32	36%
Reused Panels	164	94	86.5%	155	100	87%
Void Area	36.1 m^2	72.8 m^2	13.5%	36 m^2	96 m^2	13%

As shown in Fig. 9 and Fig. 10, both scenarios achieved the same WWR on both façades despite using different quantities and window types. The uncovered area on the south façade is similar across scenarios, even though scenario 2 uses fewer panels than scenario 1. Scenario 1 achieves a greater covered area on the north façade than scenario 2 despite using fewer panels.

After distributing reused panels on the south and north façades, the process continued with a second optimization to select insulation materials for the ground floor, exterior walls, and roof. The goal was to minimize the GWP over the building's life cycle. To make the U-values of the envelope surfaces match the pre-optimized values (equality constraint) and ensure the insulation thickness did not exceed 0.55 m (inequality constraint), the PGDS conducted a brute force search of all available insulation materials in Bombyx for each building envelope surface. The search excluded natural-based insulation materials for the ground floor for the same reasons presented in section 4.1.

Table 10 presents the final operational and GWP results of experiment 2.

Table 10. Insulation material selection, EUI, and GWP results of experiment 2.

	Scenario 1: 60-10% WWR	Scenario 2: 60-10% WWR
Insulation Material		
Ground floor	Rockwool board (thickness: 340mm)	Rockwool board (thickness: 340mm)
External Walls	Cellulose batt (thickness: 520mm)	Cellulose batt (thickness: 520mm)
Roof	Flax fiber boards (thickness: 440mm)	Flax fiber boards (thickness: 440mm)
EUI (kWh/m^2year)	104	104
GWP (reusing materials) (kg CO_2/m^2year)	10.9	11
GWP (new materials) (kg CO_2/m^2year)	11.8	11.9

5 Discussion

The following discusses the results of both experiments regarding the PGDS's potential to help reassemble reclaimed building materials and parts and minimize building carbon emissions.

5.1 Reassembling reused material

The PGDS's ability to maximize the use of reclaimed building materials supports the reduction of material waste and the need for new materials in façade cladding. The results show that the gaps between reused materials depend on the size and quantity of available panels and the degree of regularity of façade composition. For example, because the façade area to clad presents some shape irregularities and the experiments started with allocating reused building parts in the south façade, fewer smaller panels could adjust to the shape complexity of the north façade. A potential solution is not controlling the window placement to allow better overall packing of the different façade elements. Alternatively, it is possible to further break larger panels, available in the material atlas, into smaller parts. Nevertheless, disassembling existing buildings into smaller parts requires more effort, time, and resources, leading to increased carbon emissions. Therefore, it is necessary to carefully evaluate the tradeoffs between the disassembling processes, the size of resulting parts, and their potential use in reassembly. Additionally, combining certain window types into larger units on the south façade created more regular areas for panel placement, making packing easier. This strategy was not applied on the north façade in experiment 2 due to the lower WWR and reduced glazing needs.

In sum, to improve future outcomes, the proposed approach needs to balance three key aspects: (i) distribution of WWR percentage between façades, (ii) positioning of windows considering the dimensions of cladding elements to minimize non-covered area, and (iii) dimensioning the post-processing of reused material at the disassembly phase to maximize reused material usage.

5.2 Environmental impacts assessment

The two experiments showed the PGDS's ability to support different approaches to low-carbon architecture. The framework seamlessly integrated operational energy key performance indicators (e.g., EUI) with GWP LCA calculations. The experiments focused on assessing the benefits of reusing building waste for façade cladding and selecting thermal insulation materials to reduce the overall GWP of new buildings. The PGDS facilitated GWP calculations in both experiments while balancing other relevant indicators, such as EUI and façade U-value.

In experiment 1, the iterative manual study revealed an 18% potential savings in GWP (kg CO2/m2/year) between the least (façades with a WWR 40-40% distribution, XPS insulation, and new materials in cladding) and the best-performing solution (façades with a WWR 50-30% distribution, cellulose

insulation, and reused materials in cladding). When comparing the two versions of each design solution, i.e., either using reused or only new materials, the savings in GWP are from 8 to 12%. These modest results relate to the surface area targeted for reused material application, which is ≈ 20% of the total building surface area, including interior and exterior building surfaces. Additionally, the authors observed that operational energy was the largest contributor to GWP, representing 70 to 85% of total GWP emissions.

Experiment 2 involved pre-optimizing the building's shape, WWR, and the thermal resistance of the façades to reduce operational energy, the primary contributor to GWP observed in experiment 1. The optimization prioritized maximizing solar gains by increasing the length of the façades and the south façade WWR while minimizing transmission losses by reducing the WWR on the north façade and minimizing the façades' U-values, a design strategy adequate for the Danish climate. Despite improving the EUI by approximately 10 to 12% compared to experiment 1, the allocation of reused material was slightly less efficient. Nevertheless, the results of experiment 2 outperformed the best-performing solutions found by experiment 1's manual iterative process - 5% better than the best solution and 22% better than the least-performing one. Such results demonstrate the value of integrating search and optimization processes into the design workflow. Finally, the difference in GWP performance between the two design scenarios in experiment 2 is negligible, indicating the PGDS optimization module robustness.

6 Conclusion

The research addressed challenges in circularity within the design process by proposing a framework that integrates computational design, Life-Cycle Assessment (LCA), and Building Energy Simulation (BES) to support the creation of low-carbon buildings. This framework resulted in a Performance-based Generative Design System (PGDS) that promotes the reuse of demolition waste and helps architects design energy-efficient, low-carbon buildings with a waste-conscious approach. The paper detailed the PGDS structure, supported workflows, and assessed its effectiveness in optimizing building elements, improving energy consumption, and evaluating the environmental impact of different design solutions through two design experiments in Horsens, Denmark.

The results demonstrated the PGDS's ability to integrate circular economy principles into the design process by combining design-specific requirements with element packing techniques. The system supports balanced design investigations between the tectonic expression of building façades and waste reduction in construction by maximizing the reuse of building parts. Unlike traditional packing, which prioritizes space efficiency over design diversity, the PGDS accommodates aesthetic and performance criteria. For instance, it enables setting zones for window placement and restricting materials in areas with specific design requirements, fostering varied yet cohesive material arrangement.

Nevertheless, the allocation of reused material is currently limited to rectangular surfaces, and the packing algorithm only supports square or rectangular elements. Expanding these capabilities to support more varied surface geometries would increase flexibility and enhance design possibilities. Additionally, automating cutting strategies of panels from reused building materials would improve architectural design adaptability. Future improvements could also involve assigning specific panel types to different façade sections to optimize material usage and improve design cohesion, ensuring a controlled, efficient balance between material reuse, aesthetics, and performance.

The experiments also showed the PGDS's ability to facilitate comparative analysis and optimization of building energy performance and cradle-to-grave global warming potential (GWP). They show the PGDS's capacity to estimate the potential for reusing building materials in façades and selecting insulation materials that minimize overall GWP while balancing other critical building performance criteria, such as energy use intensity and envelope thermal resistance.

The experimental application of the PGDS's search and optimization capabilities demonstrated its potential to steer the design process toward energy and carbon efficiency. It also revealed that improving building energy efficiency may result in suboptimal WWRs and building shapes for reused material allocation. Future work will explore multi-objective optimization techniques to further investigate potential tradeoffs between maximizing material reuse and minimizing building energy and cradle-to-grave GWP. Additionally, future developments will integrate the assessment of key indoor environmental quality indicators, such as thermal comfort, visual comfort, and daylight availability, to ensure a holistic approach to low-carbon building design.

Acknowledgements

The authors thank Azul Isidoro, Bastian Mosegård, and Nicolai Thomsen for providing the application case study and material atlas. Special thanks to Ramus Nørulf for the invaluable help in rendering some solutions. Additionally, we sincerely thank Azul for the valuable insights on LCA application in the Danish context. Thanks to Aalborg University's section of Architecture and Urban Design for sponsoring the presentation of this work at the 7th Formal Methods in Architecture symposium. This work was also supported by Portuguese national funds through Fundação para a Ciência e a Tecnologia (FCT) with reference DOI: 10.54499/UIDB/50021/2020.

References

1. A Acevedo-De-los-Ríos, "Building Materials and the Climate: Constructing a New Future.," 2023. Accessed: Nov. 15, 2024. [Online]. Available: https://dial.uclouvain.be/pr/boreal/object/boreal:285383

2. B Goldstein and FN Rasmussen, “LCA of Buildings and the Built Environment,” in *Life Cycle Assessment*, M. Z. Hauschild, R. K. Rosenbaum, and S. I. Olsen, Eds., Cham: Springer International Publishing, 2018, pp. 695–722. doi: 10.1007/978-3-319-56475-3_28.
3. K Ostapska, P Rüther, A Loli, and K Gradeci, “Design for Disassembly: A systematic scoping review and analysis of built structures Designed for Disassembly,” *Sustainable Production and Consumption*, vol. 48, pp. 377–395, Jul. 2024, doi: 10.1016/j.spc.2024.05.014.
4. U Kozminska, “Circular design: reused materials and the future reuse of building elements in architecture. Process, challenges and case studies,” in *IOP Conference Series: Earth and Environmental Science*, IOP Publishing, 2019, p. 012033. Accessed: Nov. 15, 2024. [Online]. Available: https://iopscience.iop.org/article/10.1088/1755-1315/225/1/012033/meta
5. M Condotta and E Zatta, “Reuse of building elements in the architectural practice and the European regulatory context: Inconsistencies and possible improvements,” *Journal of Cleaner Production*, vol. 318, p. 128413, 2021.
6. K Rybak-Niedziółka *et al.*, “Use of waste building materials in architecture and urban planning—a review of selected examples,” *Sustainability*, vol. 15, no. 6, p. 5047, 2023.
7. M Moreno, C De los Rios, Z Rowe, and F Charnley, “A conceptual framework for circular design,” *Sustainability*, vol. 8, no. 9, p. 937, 2016.
8. M Yadav and M Agarwal, “Biobased building materials for sustainable future: An overview,” *Materials Today: Proceedings*, vol. 43, pp. 2895–2902, 2021.
9. B Yang, Q Wang, and SS Man, “Sustainable Material Innovation Design for Building Construction: Exploring Bio-Based Alternatives,” in *Frontiers in Artificial Intelligence and Applications*, L. C. Jain, V. E. Balas, Q. Wu, and F. Shi, Eds., IOS Press, 2024. doi: 10.3233/FAIA231427.
10. “En Naturlig Pavillon,” Reværk Arkitektur. Accessed: Nov. 15, 2024. [Online]. Available: https://revaerk.dk/en-naturlig-pavillon/
11. MR Skov, “BIOSACK | Michael Rex Skov Arkitekter.” Accessed: Nov. 15, 2024. [Online]. Available: https://rexskov.dk/project/biosack-2/
12. W Debacker and S Manshoven, “State of the art, Key barriers and opportunities for Materials Passports and Reversible Building Design in the current system,” *Synthesis report*, no. D1, 2016.
13. S Basic, A Hollberg, A Galimshina, and G Habert, “A design integrated parametric tool for real-time Life Cycle Assessment–Bombyx project,” in *IOP conference series: earth and environmental science*, IOP Publishing, 2019, p. 012112. Accessed: Nov. 15, 2024. [Online]. Available: https://iopscience.iop.org/article/10.1088/1755-1315/323/1/012112/meta
14. F Heisel and C Nelson, “RhinoCircular: development and testing of a circularity indicator tool for application in early design phases and architectural education,” in *AIA/ACSA intersections res conference: CARBON*, 2020, pp. 154–159. Accessed: Nov. 15, 2024. [Online]. Available: https://www.researchgate.net/profile/Felix-Heisel/publication/346678011_RhinoCircular_Development_and_Testing_of_a_Circularity_Indicator_Tool_for_Application_in_Early_Design_Phases_and_Architectural_Education/links/5fce2c5292851c00f858e842/RhinoCircular-Development-and-Testing-of-a-Circularity-Indicator-Tool-for-Application-in-Early-Design-Phases-and-Architectural-Education.pdf
15. “ISO 21930: 2017 Sustainability in buildings and civil engineering works – Core rules for environmental product declarations of construction products and services.” 2017.

16. “EN 15804: 2012 + A2:2019 Sustainability of construction works. Environmental product declarations. Core rules for the product category of construction products.” 2019.
17. E Commission, “PEFCR Guidance Document- Guidance for the Development of Product Environmental Footprint Category Rules (PEFCRs), Version 6.3.” Publications Office of the European Union Luxembourg, 2017.
18. “Circular[X]Change,” Circular[X]Change. Accessed: Nov. 15, 2024. [Online]. Available: https://www.cxc-europe.eu
19. M Sammer, A Leitão, and I Caetano, “From visual input to visual output in textual programming,” in *Proceedings of the 24th International Conference of the Association for Computer-Aided Architectural Design Research in Asia (CAADRIA)*, 2019, pp. 645–654. Accessed: Nov. 18, 2024. [Online]. Available: https://papers.cumincad.org/data/works/att/2019_CAADRIA_volume1.screen.pdf#page=661
20. DB Crawley *et al.*, “EnergyPlus: creating a new-generation building energy simulation program,” *Energy and buildings*, vol. 33, no. 4, pp. 319–331, 2001.
21. RL Harrison, “Introduction to monte carlo simulation,” in *AIP conference proceedings*, NIH Public Access, 2010, p. 17. Accessed: Nov. 18, 2024. [Online]. Available: https://www.ncbi.nlm.nih.gov/pmc/articles/PMC2924739/
22. Sollema LLC, “Climate Studio.” Accessed: Jul. 27, 2020. [Online]. Available: https://www.solemma.com/ClimateStudio.html
23. “Metaheuristics.jl · Optimization.jl.” Accessed: Nov. 18, 2024. [Online]. Available: https://docs.sciml.ai/Optimization/stable/optimization_packages/metaheuristics/
24. A Isidoro, B Mosegård, and N Thomsen, “Sundparken: Building Circularity in Social Housing,” Master’s Thesis, Aalborg University, Department of Architecture, Design and Media Technology, 2023. Accessed: Oct. 31, 2024. [Online]. Available: https://projekter.aau.dk/projekter/files/538494000/MSc04_ARC_G2_Sundparken_Sourcing__Reuse_and_Transformation_spreads_compressed_compressed__1_.pdf
25. FCS Liu, SC Lin, J-Y You, Y-T Chen, and J-L Sun, “From Internal Validation to Sensitivity Test: How Grid Computing Facilitates the Construction of an Agent-Based Simulation in Social Sciences,” in *Proceedings of The International Symposium on Grids and Clouds and the Open Grid Forum — PoS(ISGC 2011 & OGF 31)*, Academia Sinica, Taipei, Taiwan: Sissa Medialab, Sep. 2011, p. 002. doi: 10.22323/1.133.0002.
26. “Key figures,” The Danish Energy Agency. Accessed: Nov. 19, 2024. [Online]. Available: https://ens.dk/en/our-services/statistics-data-key-figures-and-energy-maps/key-figures
27. ASHRAE, “ASHRAE Standard 90.1-2013 Determination of Energy Savings: Quantitative Analysis.” 2013.
28. S Sayadi, A Hayati, and M Salmanzadeh, “Optimization of window-to-wall ratio for buildings located in different climates: An IDA-indoor climate and energy simulation study,” *Energies*, vol. 14, no. 7, p. 1974, 2021.